Surveys in Geophysics (2018) 39:1149–1166
https://doi.org/10.1007/s10712-018-9484-0

Geophysical Methods and Spatial Information for the Analysis of Decaying Frescoes

Maria Danese[1] · **Maria Sileo**[1] · **Nicola Masini**[1]

Received: 15 February 2018 / Accepted: 21 June 2018 / Published online: 18 July 2018

Abstract
A promising application field of geophysics is monitoring and analysis of the state of conservation of works of art, such as wall paintings including frescoes. To this aim, two are the issues to address: the choice of the most appropriate survey instrument and method, and the analysis and interpretation of data coming from the survey, after their processing. This paper deals with a spatial analysis based protocol for the interpretation of data coming from different non-invasive tests, to improve the extraction process of the pattern decay. The case study is a frescoed wall of Gymnasium in Pompeii, investigated with the following non-invasive techniques: structure-from-motion photogrammetry (SfM), ground-penetrating radar, multitemporal infrared thermography.

Keywords Fresco · DEM · Multitemporal infrared thermography · GPR · Spatial analysis

1 Introduction

In recent years the use of geophysics for cultural and archaeological heritage increased covering different applications including risk monitoring, preventive and rescue archaeology (Conyers 2004; Goodman and Piro 2013), diagnosis of the state of conservation of architectural monuments (Pérez-Gracia et al. 2013; Leucci et al. 2011; Masini et al. 2010) and works of arts such as rose windows, mosaics and wall paintings (Masini et al. 2007). This was due to the improvement of sensors and data processing tools as well as the increased awareness of the need to investigate cultural heritage assets with non-invasive technologies (Masini and Soldovieri 2017).

✉ Maria Danese
m.danese@ibam.cnr.it

Maria Sileo
m.sileo@ibam.cnr.it

Nicola Masini
n.masini@ibam.cnr.it

[1] CNR-IBAM, Contrada S. Loja, Zona Industriale, Tito Scalo, PZ 85050, Italy

This last aspect is fundamental for the frescoes as they are extremely fragile cultural heritage and more exposed to the risk of deterioration and destruction as in this case. Consequently, preventive conservation is a priority action, to minimize the progress of degradation and to minimize the costs necessary for future restoration and to to extend its lifetime (Merello et al. 2016). The understanding of the conservation status of works of art must include several information, including the constituent materials of artefacts, the damage type as a result of the material and environmental degradation of the storage environment and their history and evolution over time. Only in this way, it is possible to plan measures for future maintenance or restoration. To preserve the artefacts in the best possible way, the use of invasive analysis techniques, that is those techniques that allow information directly in contact with the materials constituting the artefact and which can cause damage to the building itself, is less and less required. In fact, in recent years, the use of remote sensing technologies has become increasingly common; in particular, they allow to provide information on the state of conservation of materials without necessarily carrying out sampling or invasive actions.

Among these non-invasive techniques, ground-penetrating radar (GPR) (Leucci et al. 2011) and infrared thermography (IRT) are very much in use, also due to the minimization of their impact on the artwork. Their integration allow to better use their different resolution for the benefit of the evaluation of the conservation status of investigated artefacts through the spatial correlation of the information obtained from the different types of signal at the points of greatest interest. However, despite GPR and IRT being considered essential tools for the knowledge and conservation of cultural heritage, the absence of standard protocols for the analysis and interpretation of the acquired data for conservation purposes have resulted in an almost exclusively academic use and aimed at researches and highly specialized sector studies, limiting a wider use through the operators of the professions involved in the maintenance and restoration of works of art. In particular, from the data processing point of view, the integration of different techniques is the domain of researchers and technologists, experts in the field, that only through the analysis of very large data set are able to extract multitemporal and spatial patterns, which could lead to valuable information on the conservation status of the analyzed fresco.

However, in the field of conservation, often, data are interpreted by an expert in the field only with a visual inspection. A quantitative approach could surely constitute a Support Decision System for conservation. In particular, the spatial approach pursued in this paper is based on the intuition that a painted wall has its own topology, characterized by the presence of spatial patterns that can be investigated with methods coming from Geographic Information Science. With this aim, the Gymnasium frescoes in Pompeii were studied with spatial analysis applied to data coming from Structure-from-motion photogrammetry (SfM), multitemporal infrared thermography (MIRT) and GPR.

2 Case Study Description: The Frescoes of Gymnasium in Pompeii

The ancient city of Pompeii is divided into nine quarters or *Regiones* (Fiorelli 1875), each in turn containing blocks (*insulae*) that are made up of numerous buildings (domus) bordered by roads. The Regio VIII occupies the southwestern area of urban area of Pompeii and is limited (to the south) from an irregular stretch of city walls between the two ports, Porta Stabia and Porta Marina and is subdivided into seven insulae (see Fig. 1). Among the prestigious buildings, the *Regio* VIII includes palaces and public spaces such as the Triangular Forum, the Basilica, the Theater and the Sarno Baths, within which the Gymnasium

Fig. 1 Locations of the studied painting in Gymnasium in Sarno Baths (red box) in the Plan of Regio VII, Pompeii

is located. Gymnasium is one of the most significant rooms decorated by frescoes depicting athletes and fight scenes dated to 50 AD (Koloski-Ostrow 1990) within the Sarno bath which occupies most of the complex of the second *insula* of *Regio* VIII of Pompeii (for additional information, see Masini et al. 2017). The Sarno baths consist of a block of four levels built in the II century BCE. Severely damaged by the earthquake of 62 AD, the thermal rooms were still being renovated at the time of the eruption. The most significant rooms are the Frigidarium, decorated by paintings representing Sarno river (from which the name of Sarno bath) and Nilotic landscapes, and the gymnasium (Fig. 1, bottom),

The plaster stratigraphy of the fresco analyzed was obtained from the study of scientific literature and by direct observation. It is constituted by three layers. The first one is the 'intonachino" a thin white plaster layer consisting of a lime binder with crystalline calcite as one of the aggregates. The second layer (1–1.5 cm thick) is composed of gray-colored sublayers (inserted 'wet to wet') made up of a lime binder with an aggregate containing black volcanic sand and lumps of calcareous material. The under sublayer of plaster is slightly coarser than the upper layer. Finally, the third layer is the so-called arriccio, 3–4 cm thick, the function of which is to cling to the wall and provide a good moisture reserve for the overlying layers (Fig. 2). The Survey was conducted on the wall painting of the Gymnasium with SfM photogrammetry, MIRT and GPR.

3 Survey Methodologies

3.1 Structure-from-Motion Photogrammetry (SfM) Survey

The first survey conducted on the Gymnasium wall painting was performed by processing by structure-from-motion method multiple partially overlapped images taken using a Nikon D90, with a lens NIKKOR NIKON 18-55 AF-S Dx and a resolution of 12.3 Megapixel. The processing included the following steps: (1) the selection and loading of photos, captured with correct overlap requirement (60% of side overlap + 80% of forward overlap)

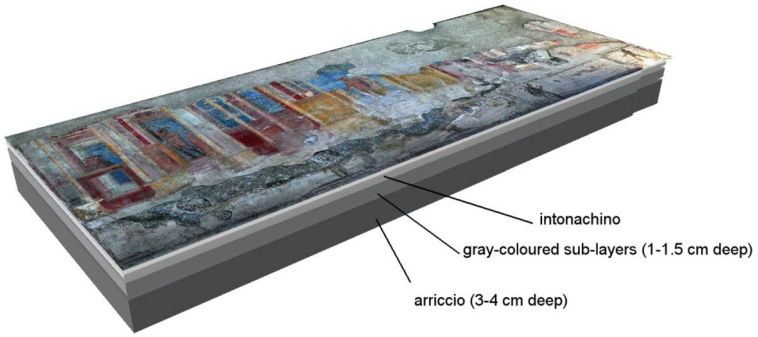

Fig. 2 Stratigraphy of the Gymnasium fresco

aimed at minimizing blind zones; (2) computation of camera position and orientation for each photo; (3) alignment of photos and building of a sparse point cloud; (4) generation of dense point cloud model which allows to calculate depth information for each camera position, (5) building of 3D model polygonal mesh; and (6) textured 3D model. The final results have been an orthophoto and a Digital Relief Model (DRM) of the walls, as showed in Fig. 3b, c, respectively.

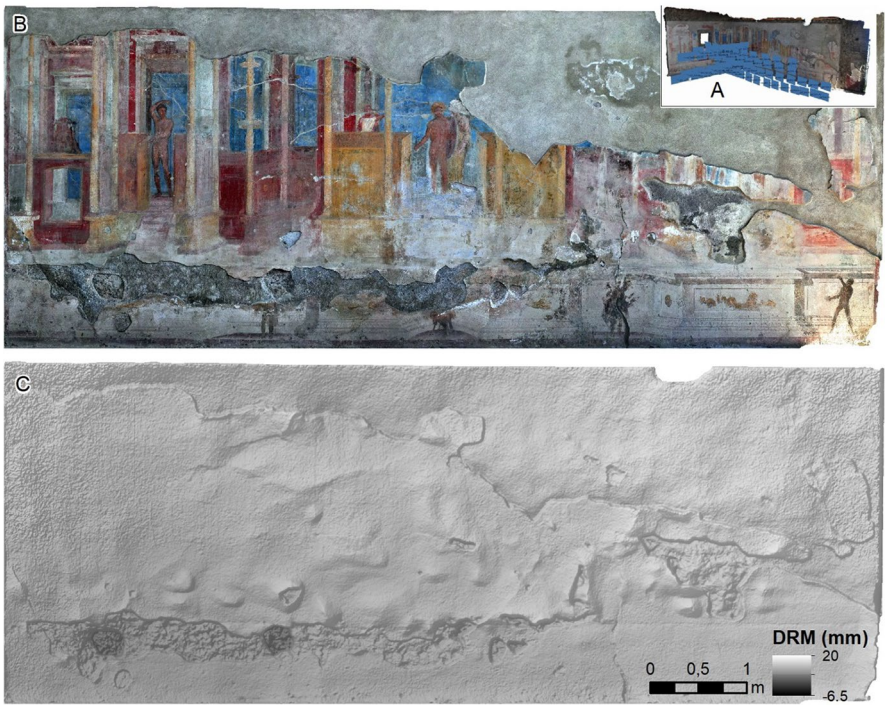

Fig. 3 3D mesh and textured model (**a**) for the extraction of the red/green/blue (RGB) (**b**) and the DRM (**c**) of the Gymnasium wall. A visualization relief technique based on shading effect was applied to DRM thus evidencing some decay pathologies such as lacks and swelling

Table 1 Types of damage and their extensions found with the visual inspection

Code	Damage definition	Areas detected with visual interpretation (square meters)
0	Areas with the best state of conservation of the fresco	17.99
	Superficial decay:	
1	Salts	0.73
	Damage interesting all the stratigraphy, from the paint layer to deeper layers:	
2	Swelling	0.46
3	Detachment	0.89
4	Fracturing	0.65
5	Lack	10.55
6	Deep lack	0.15

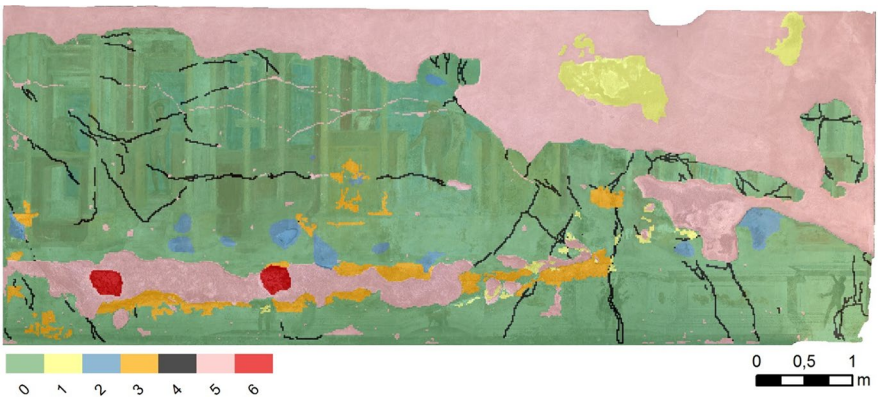

Fig. 4 Visual interpretation of decay patterns

Even if this survey was conducted on the walls located at South and East, respectively, the analysis presented in this paper was conducted only on the fresco over the East wall. The files obtained have, respectively, a spatial resolution of 0.77 mm for the orthophoto and 1.74 mm for the DRM. A true color orthophoto of the paintings is particularly useful for a first visual inspection of the wall, but also for a validation of results obtained by the analysis of DRM, and results of GPR and MIRT, to identify and map the typical decay pathologies of paintings such as biological patinas, deposits, lacks and efflorescence (salt coating). The decay patterns showed in Table 1 and Fig. 4 were obtained.

3.2 GPR Survey

The GPR is a non-invasive geophysical method that allows us to obtain electromagnetic reflections of the subsoil and of the wall structures to know the internal structure and determine the stratifications of both the subsoil and the masonry (plaster thickness, presence and location of decay pathologies such as detachments, voids, fractures or defects). Therefore, the diffusion of this technology is increasingly appreciated above all as a diagnostic tool aimed at the

knowledge, conservation and planning of restoration actions and the maintenance of cultural heritage.

The GPR equipment consists of a pair of antennas, an emitter that emits electromagnetic impulses in the investigated medium (subsoil, masonry or fresco, as in this case), and a receiver that collects the echoes of the refracted radar. The frequency of the antenna typically used on masonry is usually in the frequency range of 800–2000 MHz and allows to investigate supports with variable thicknesses from 1 m up to the detailed analysis of stratifications even in the order of a few centimetres, as in case of investigations on plasters and frescoes.

Among the fundamental aspects that must be considered during the signal processing phase is the evaluation of the physical properties of the investigated medium, in particular the determination of the transmission speed of the electromagnetic waves in the specific medium (Persico 2014). The speed evaluation phase is a fundamental step, because it allows to identify, among other things, internal reflections on the interfaces that separate the supports with different electromagnetic properties (dielectric permittivity, electrical conductivity and magnetic permeability) and to establish the characteristics of the object investigated as for example the thickness of the masonry or plaster, the presence of reflectors associated with the presence of anomalies such as voids, cracks and fractures (Persico 2014). The estimation of the EM wave speed allows the conversion of time in depth along the radar profile. With the use of GPR, it is possible to determine the presence of interfaces between different layers of the masonry, such as the wall stratifications that represent the ancient Roman walls made of opus coementicium (Lancaster 2015) or identify the presence of local reflectors associated with inhomogeneities, voids or fractures. If the medium investigated presents humidity, an increase in conductivity is generated which in turn determines a high absorption of the EM waves, in this way the information of the investigated medium is shielded; therefore, it is preferable to perform the survey in dry periods. The interpretation of the images obtained from the single radargrams can be integrated using tomographic techniques, which allow to obtain high resolution images in which the presence of anomalies is easily detected, this method is often used both for archaeological applications (Soldovieri and Orlando 2009) that for diagnostic investigations on historical monuments (Leucci et al. 2011). A more effective visualization is also given by 3D reconstructions of the georadar results, this visualization allows to obtain the reconstruction of anomalies in space and can help in the identification of strong reflectors as large inhomogeneities and voids but at the same time it is difficult to identify fractures or small anomalies that may occur in the presence of weak reflections, whose presence is detectable only through a careful analysis of individual radargrams. In this work, GPR investigations were made using the Hi-Mod IDS instrument with a 2 GHz frequency antenna. Data acquisition was made possible by interposing a plastic panel between the instrument and the surface of the frescoed wall, while the acquisition was carried out by moving the antenna in a horizontal direction. GPR data were acquired using a manual gain function with a scan of 512 samples for a 30 ns recording window. The spacing between the different horizontal strips was 20 cm (Fig. 5) for a maximal length of the longitudinal profiles equal to 5 m and up to 0.8–1.0 m of height starting from 1 m from the floor. The velocity in the middle of the electromagnetic wave was estimated at 0.10 m/ns.

3.3 Multitemporal InfraRed Thermography (MIRT) Survey

Infrared thermography (IRT) is a non-destructive NDT remote sensing technique capable of detecting infrared radiation emitted by objects with a temperature above 0 K. The infrared camera in fact transforms the value of energy emitted by a body into a temperature value

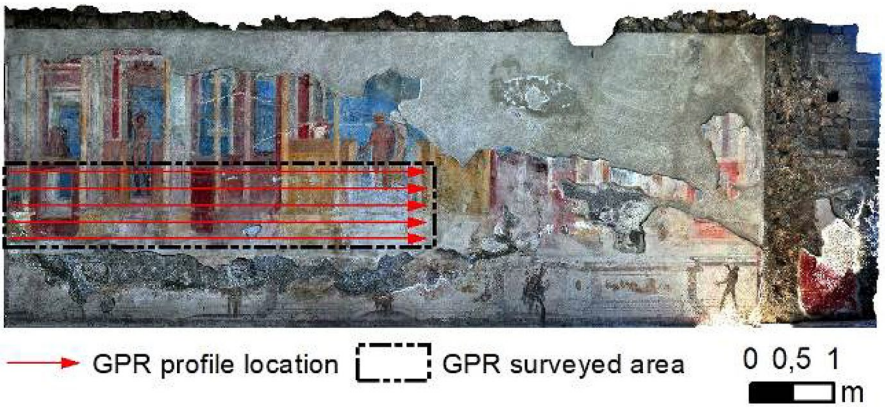

Fig. 5 Location of GPR profiles on the frescoes

through the Stefan–Boltzmann law. However, the temperature obtained by IRT and consequently the energy emitted by the surface depends on several factors such as spectral properties (emissivity, reflection), thermal properties (conductivity, specific heat, diffusivity) and other physical properties concerning the object under investigation. As the water content, porosity and density (Dumoulin 2016), IRT is widely applied to cultural heritage for different purposes such as preservation and restoration of monuments and historical sites (Faella et al. 2012) or conservations of frescoes (Bodnar et al. 2012; Candoré et al. 2010; Grinzato et al. 2002a) and is often applied accompanied to other types of invasive investigations and not, as sonic and ultrasonic techniques (Kandemir-Yucel et al. 2007), GPR (Faella et al. 2012), geoelectric (Carlomagno et al. 2011). Using IRT it is possible to map areas in the presence of moisture, detect voids and shallow surface defects and evaluate conservation treatments in a qualitative way both through a passive and active method. In particular the passive technique is mostly used for the detection of shallow subsurface voids and defects of architectural surfaces (Inagaki et al. 1999), to map moisture (Grinzato et al. 2002b) and to evaluate conservation treatments (Avdelidis and Moropoulou 2004). In the passive method used for this work, the temperature is monitored after transient solar radiation induced on the walls of the building (Grinzato et al. 1998).

In this work, the imaging of frescoes was made using an FLIR SC660 with FPA detector (Focal Plane Array) uncooled microbolometer operating in the spectral range between 7.5 and 13 14 μm. The survey was carried out on 21/04/2015 in the afternoon (after 02:30 pm) with a distance from the frescoed wall of about 3 m and with external temperature of 26,6 °C and a relative humidity of 88,0%. Three thermograms were taken, having a spatial resolution of 1.51 cm and a time resolution of 8 min. From here, we referred to t0 at the first thermogram taken at the time 0, with t8′ to the thermogram taken after 8 min and with t16′ to the thermogram taken after other 8 min.

4 Analysis Methodologies: Spatial Analysis Based Approach

In this paper, the fresco was considered as a vertical geographical space, even if an improper one. Different type of spatial analysis was used to extract information from the RGB, the DRM, the MIRT and the GPR data.

Spatial analysis studies the spatial distribution of phenomena, aggregation shapes and existing relationships, by considering their heterogeneity and their mutual dependency as indicated by spatial autocorrelation. Presence of autocorrelation in one variable causes a variation of the spatial distribution; under hypothesis of complete spatial randomness, in the case of events completely independent each other, this distribution would be different. A spatial distribution can be affected by two factors: (1) first order effects, related to region properties, are expressed by the spatial variation in the expected value (mean) of events and (2) second order effects, related to local interactions between events, are instead expressed by the spatial variation of covariance. The presence of first and second order effects cause the spatial autocorrelation in the distribution, that can assume three different types of configuration: (a) there's a positive spatial autocorrelation or attraction between events when points are concentrated in clusters (clustered distribution); (b) there's negative spatial autocorrelation or repulsion, when events are near in the space but they have different quantitative properties, so it is impossible to find homogeneous areas (uniform or regular distribution); (c) there's null autocorrelation (random distribution) when it is not possible to find any spatial effects, both for what concern spatial location, both for what concern properties of each event. Consequently, when null autocorrelation is verified events have a random spatial distribution; so in this case the complete randomness hypothesis' is verified. Spatial methods used are map algebra, hotspot analysis and geovisual analytics.

4.1 Map Algebra

Map Algebra is an important instrument for data preprocessing or for evaluating in the simplest way areas characterized by homogeneity of a chosen parameter. It is a high level language for spatial modelling; it comprises simple basic elements (operators), more complex elements (functions), a formal language (instructions) and all needed elements to program and to develop complex models (De Mers 2002). According to the literature, it is based on local, focal and zonal (Tomlin 1990) functions that, mixed together, allow constructing personal functions or personalized computation. In addition, surface analysis used to study relief variations are based on map algebra.

4.2 Hotspot Analysis

Hotspot analysis allows us to better understand distribution of existing data, by finding, with the research of spatial autocorrelation, areas, where there are group of pixels with local anomalies. In the case of a fresco, the presence of autocorrelation indicates the similarity properties of materials, such as its conservation state or beforehand the type of constituting material. It can be very useful for analyzing data coming from IRT or GPR, because it allows not only considering the single pixel value, but also the relationships between its surrounding. In particular the index used was the Getis and Ord's Gi (1992), defined according to formula (1):

$$G_i(d) = \frac{\sum_{i=1}^{n} w_i(d)\, x_i - x_i \sum_{i=1}^{n} \bar{w}_i(d)}{S(i)\sqrt{\left[(N-1)\sum_{i=1}^{n} w_i(d) - \left(\sum_{i=1}^{n} w_i(d)\right)^2\right] \Big/ N-2}}, \tag{1}$$

where N is the total pixel number, x_i and x_j are intensity in i and j points (with $i \neq j$), $\bar{X}$ is the average value. w_{ij} is an element of a weight matrix; this is used to conceptualize spatial

and quantitative relationships between events studied, that is to model distances and contiguity and influences between events (For a deepening on weight matrix meaning and construction see O'Sullivan and Unwin 2002). Finally, S is the variance.

If the G and the intensity value are simultaneously high, there is high positive autocorrelation, while if the G and the intensity value are simultaneously low there is low positive autocorrelation.

4.3 Geovisual Analytics

Geovisual analytics allows us to explore, reduce and return prediction with techniques coming from visual data mining of geospatial information (Keim and Ward 2003) with the help and at the same time by improving the human visual ability to find patterns (MacEachren and Kraak 2001). It is part of geovisualization and includes different disciplines, such as geographic information science, image analysis and exploratory data analysis (Andrienko et al. 2007a). Geovisual analytics allows us to conduct image analysis by considering together the geographic dimension and the multidimensionality coming from heterogeneous information, to reduce the analysis complexity and the quantity of data processed (Andrienko et al. 2007b). The final aim is doing pattern extraction, in our case decay patterns that, applied to a data set such as IRT or GPR allow to deepen a study based on the visual interpretation.

In this work, the V-analytics software was used (Andrienko and Andrienko 2005) to perform the Self-organizing Maps (SOM) (Kohonen 1997). The self-organizing maps is a neural network architecture that allows reducing the n-dimensionality of the input data in a two-dimensional lattice. At the same time, it maintains topological relationships of the original data set. Through a learning algorithm, without supervision, it is useful for pattern extraction. The colors of the SOM cells show similarity between events, while the black to white color between cells shows distances between clusters.

5 Results

5.1 RGB Layer Analysis

The acquisition of colors is usually in red, green and blue (RGB) components, even if probably this is not the better representation for the image classification, due to the correlation between these three bands (Guarnieri et al. 2014). (Rangayyan et al. 2011) suggests a type of representation closer to the human visual system, the HIS or HSV system, based on: hue (H), related to the dominant wavelength in the color (expressed as degree), saturation (S), connected to the color purity (%) and intensity (V), that is the brightness of the color, measured as its spectral definition (%). By considering R', G', B' are the R, G and B band expressed from 0 to 1:

$$V = M = \max\left(R', G', B'\right)$$

$$m = \min\left(R', G', B'\right)$$

$$C = M - m$$

$$H = \begin{cases} 0^{\circ}, & \text{if } C = 0 \\ 60^{\circ} \times \frac{G'-B'}{C} & \text{if } M = R' \\ 60^{\circ} \times \left(\frac{B'-R'}{C} + 2\right) & \text{if } M = G' \\ 60^{\circ} \times \left(\frac{R'-G'}{C} + 4\right) & \text{if } M = B' \end{cases}$$

$$S = \begin{cases} 0 & M = 0 \\ \frac{C}{M} & M \neq 0 \end{cases}.$$

The RGB obtained with SfM was converted through map algebra in HSV. The V component (areas with $V \geq 0.85$) was useful for the extraction of salts over the paintings (Fig. 6), while the efflorescence over the wall of the fresco already detached were found with MIRT processing showed further.

Moreover, the V raster was analyzed with hotspot analysis, using as intensity the V value, Euclidean distance and the Distance bandwidth as methods for calculation of distances, proximity and weights matrixes. As distance bandwidth a spatial lag of 2 was used, as appropriate for hotspot analysis conducted over a raster (Lanorte et al. 2013; Nolè et al. 2014). The results show that moving to the right of the fresco (green areas) there is a progressive phenomenon of decoloration of the existing pictorial pigments, due a major exposure to the Sun and external agents (Fig. 7). The H raster instead is useful to highlight areas with local detachment of pigments (Fig. 8).

5.2 Digital Relief Model (DRM) Analysis

The DRM was analyzed with basic methods taken from geomorphometry that is contour and slope analysis. By executing contouring with 0.2 mm of contour interval, by classifying it in

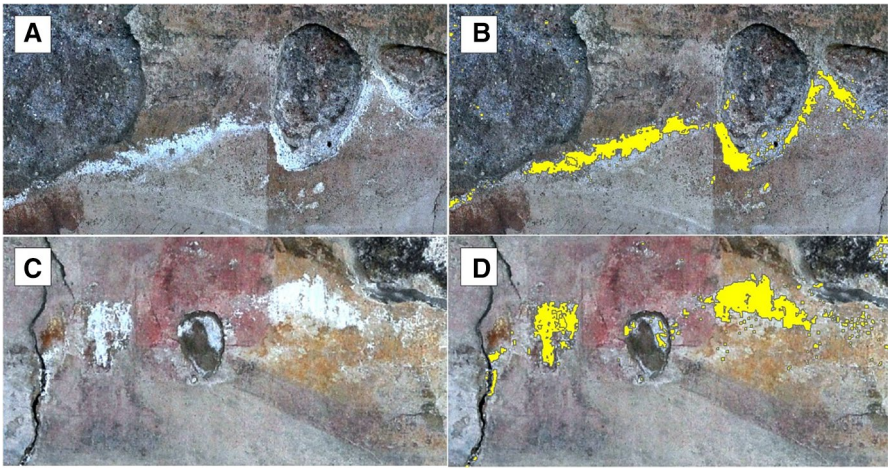

Fig. 6 Salt pattern extraction, two details (**a**, **c**) of the fresco with the corresponding distribution of salts found (in yellow **b**, **d**)

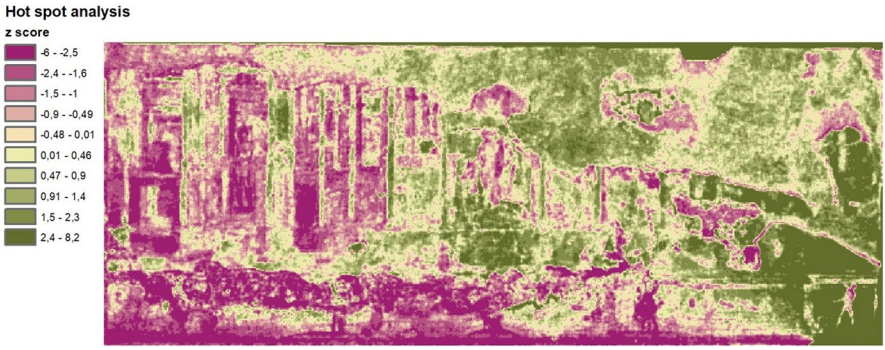

Fig. 7 Hotspot analysis for V raster. Green areas shows the progressive phenomenon of decoloration of the existing pictorial pigments

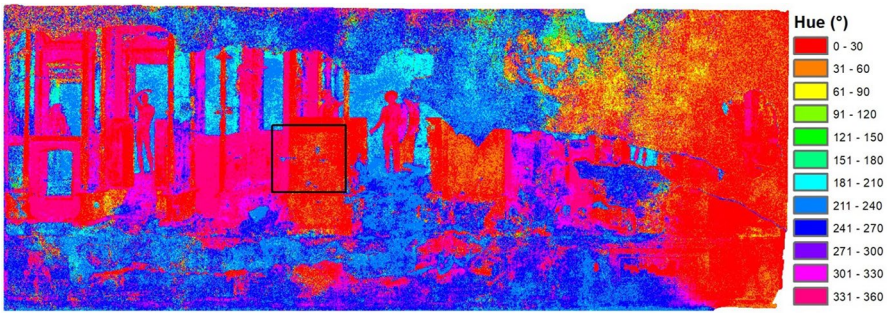

Fig. 8 Dominant color of pigments (H) highlights areas with local pigment detachment, as in the drawn rectangle

quantiles, after the elimination of outliers and by converting close lines in polygons it was possible to extract swellings, detachments and lacks (Fig. 9). In particular lacks at three different depths were detected, one that corresponds to the deep lack individualized also in the visual interpretation, one less deep called medium lack and finally one more superficial called surface lack. Moreover, the strongest fracturings are extracted even if it is not possible to distinguish them automatically from surface lacks.

By extracting these decay features, another pattern was found at the upper left side of the paintings (in green in Fig. 9): an area characterized by intense roughness, probably due a major exposure of external agents and wind in the past when there was not a canopy covering the fresco. Finally, it is interesting to observe the behaviour of the isolines: the areas covered by the surface lack have the same "elevation" of parts of the still painted areas (the cyano and the orange classes, Fig. 10). The hypothesis is that these are the parts of the fresco, together with swelling, having a higher risk of new detachments.

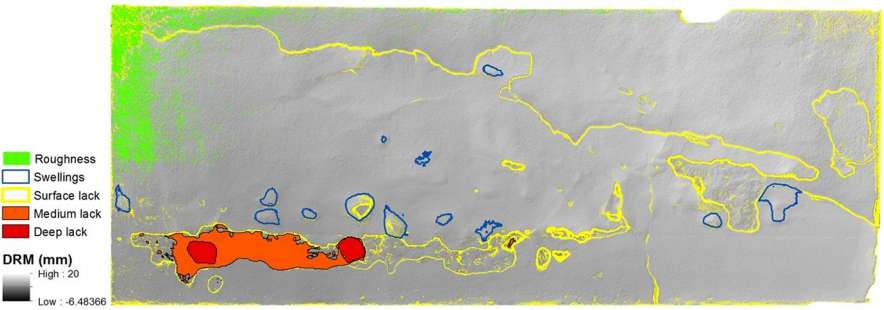

Fig. 9 Decay extraction from DRM

Fig. 10 Contouring derived from DRM. The orange and the cyano classes could reveal areas more at risk

5.3 InfraRed Thermography (IRT) Analysis

The three basic thermograms (t0′, t8′, t16′) were preprocessed with map algebra, to calculate raster representing change over time (cooling and heating) of the infrared channel. Therefore, three interval raster were obtained: t8′–t0′, t16′–t8′ and t16′–t0′. All these data, first, were simply classified in 20 quantile classes. Figure 11 (t0′, t8′, t16′) shows that the lower part of the map is the coldest one, while the interval raster (t8′–t0′, t16′–t8′ and t16′–t0′) show which are part that are getting warmer and which one are getting colder (Fig. 11).

However, both from the raw thermograms and from these differences raster, even if some patterns (lacks and the major efflorescence in the upper part of the wall) are visible, information is not so differentiate to be extracted (Fig. 11). Moreover, we want to consider at the same time similar spatial and the temporal behaviour of each pixel, to find areas characterized by a similar thermal inertia and consequently by similar properties such as constituting materials and their conservation state. Due also to the total dimension of the MIRT data set (each IRT raster is characterized by 603 (column) × 235 (raw) × 3 (number of thermograms) = 425,115 pixels) we decided to analyze them with SOM (Self-organizing Maps), partially following the approach pursued in (Danese et al. 2010). For the SOM a lattice of 5 * 3 elements was chosen.

From the result obtained first, it was possible to highlight and extract the major efflorescence in a better way than in the visual interpretation. In fact, the RGB boundaries

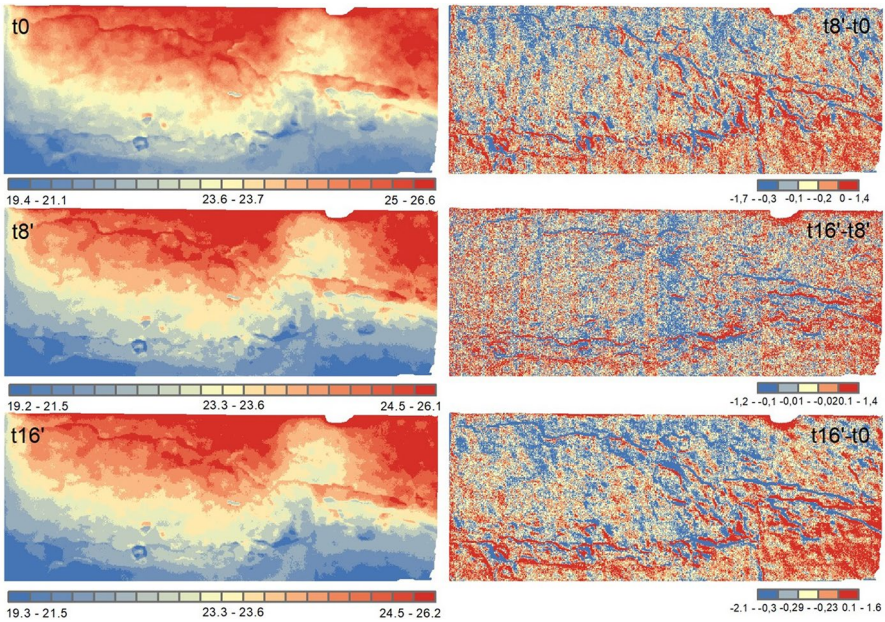

Fig. 11 Thermograms temperature (°C) classified in 10 quantiles (t0, t8′ and t16′) and differences between thermograms temperatures (°C) classified in 5 quantiles (t8′–t0, t16′–t8′, t16′–t8)

that establish the end of the phenomenon are not very clear. Second, in the upper of the wall, it is interesting to note that the boundaries of the fresco are not distinguishable from the area detached, but the cyan cluster overlays both (Fig. 12). This suggests a similar thermal behaviour. In our opinion, this similarity corroborates the hypothesis made in Sect. 5.3 according which these areas of the fresco are apparently safe, but have a significant risk of detachment. Finally, in the lower part of the wall the clusters found (in orange, red and dark violet) point out a capillary ascent phenomenon with a different severity degree.

5.4 Ground Penetrating Radar (GPR) Data Set Analysis

The GPR data set was analyzed with hotspot analysis applied to each time slice at the different depth. Again as in 5.2, the Fixed Distance Band method was used with a spatial leg of two. The method allows to evaluate adhesion between the different layers that compose the fresco stratigraphy. By evaluating at a different depths, the georadar anomalies indicate that this adhesion varies. The hotspot analysis, overlayed with damaged areas, highlights, better than the simple classification of the GPR raster, with the lower (the blue one) and the hotter (red) clusters zones characterized, respectively, by a better or worst adherence. In particular, red clusters are the same. In Fig. 13, it is possible to see how the dimension of these clustered areas varies in the different layers, at the different depths. The reliability of this type of analysis over GPR data is offered by the time slice more superficial. In fact, it shows the same anomalies visually detected with IRT.

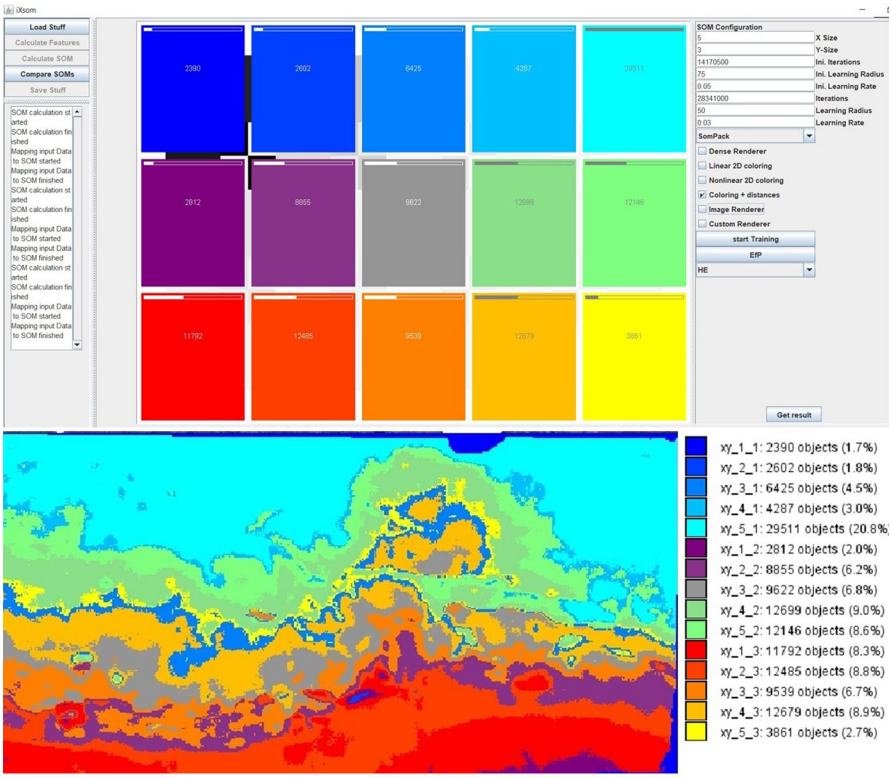

Fig. 12 Screenshot of the V-analytics with the obtained SOM and clusterization of MIRT

5.5 The Final Decay Map and Quantification

In Fig. 14, the map with the final state of conservation of the wall is reported, with all decay patterns extracted and with areas more subjected at the risk of future detachments. By comparing Fig. 14 with the visual interpretation in Fig. 4 it is possible to see how much the real state of conservation of the fresco shows a high complexity. Finally, the quantification of each pattern could be calculated (Table 2). Of course, the sum of the total cannot be equal to the total fresco surface, because there are overlays between some categories.

6 Conclusion and Further Development

The analysis of frescoes is still entrusted only to visual interpretation. The combination of a geophysical survey conducted with different instruments and of the use of spatial analysis for decay extraction and quantification can be a very useful technologies to obtain a map of its state of conservation more precise and complete also of phenomena not immediately visible only with the human eye.

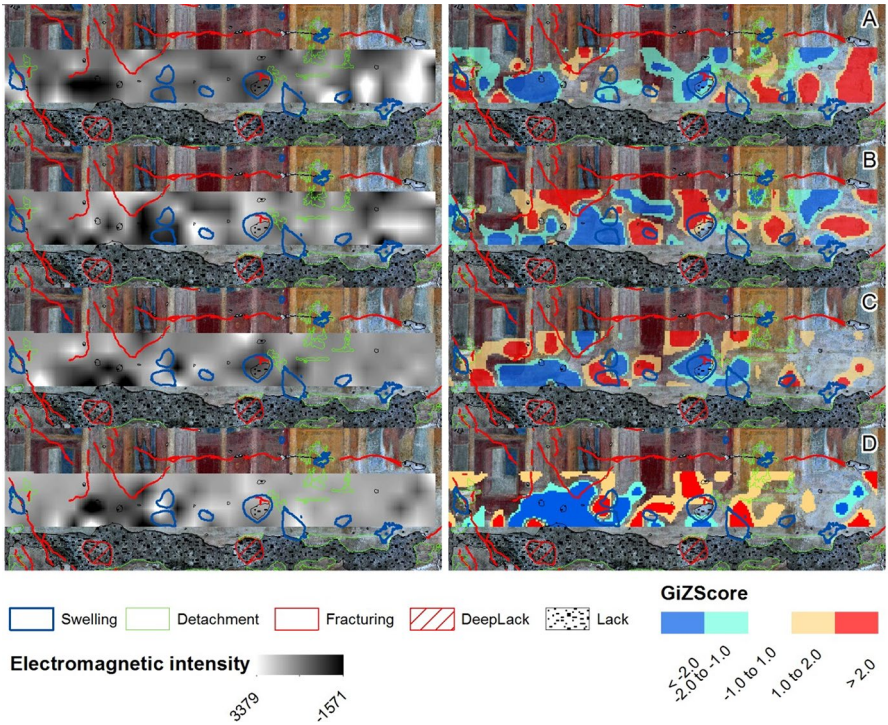

Fig. 13 GPR time slices (left column) and corresponding Getis and Ord's Gi result (right column) at the different depth: z = 2.5 mm (**a**), z = 1.5 mm (**b**), z = 3.5 mm (**c**), z = 5 mm (**d**)

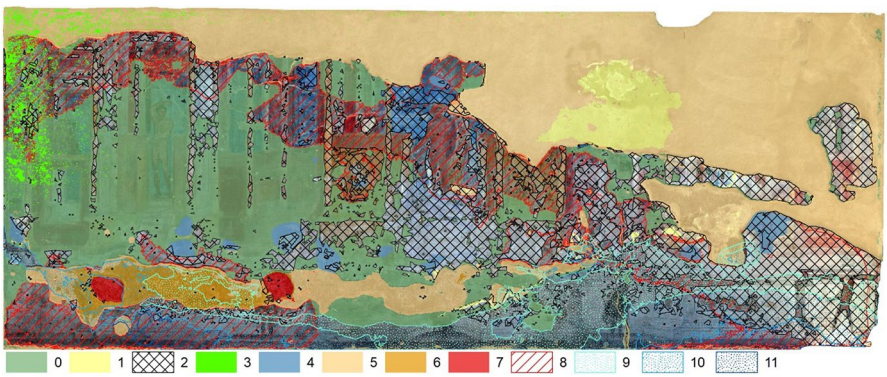

Fig. 14 The final map with decay patterns and risk areas extracted with spatial analysis

This work shows and discusses the results from an application made on some frescoes of the Gymnasium in Sarno Baths in Pompeii, based on photogrammetry, IRT and GPR. They provided a multi-dimensional data set consisting of the RGB, the DRM, the MIRT and the GPR layers. The main novelty was to treat the wall as a geographic space and the use of different types of spatial analysis.

Table 2 Types of damage and their extensions found with the spatial analysis

Code	Damage definition	Areas detected with visual interpretation (square meters)
0	Areas with the best state of conservation of the fresco	6.42
	Superficial decay:	
1	Salts	0.93
2	Areas with decoloration risk	6.62
3	Roughness	1.47
	Damage interesting all the stratigraphy, from the paint layer to deeper layers:	
4	Swelling	0.46
	Lack	
5	Surface	14.95
6	Medium	2.17
7	Deep lack	1.51
8	Areas with detachment risk	8.48
	Water capillary rising:	
9	Low	2.37
10	Medium	2.24
11	High	0.59

This approach enabled us: (1) to extract decay patters; (2) to reconstruct the 3D model, that constitutes the deformation map of the painting analysis methodology; and (3) to establish a first step for restoration of an important multilevel characterization of a fresco useful for the protection and mitigation of its deterioration risk.

However, the analysis protocol exhibits some limits and consequently needs to be further improved even adding more spatial analysis. For example, one limit checked was the fracturing extraction, not possible with neither of the instrument or analysis used; in fact, only larger fractures are extracted as it is possible to see in Fig. 14 and, however, only as surface lack areas.

Another limit regards the different spatial resolution of the layers obtained with the used survey techniques (DRM, RGB, GPR and MIRT). The change of cell size affects spatial analysis in terms of accuracy of the results, so it is desirable a further study where to deepening this aspect. With this aim, all techniques used in this work should be systematically applied on different spatial resolution for the same type of layer and results compared and validated to find a theoretical optimal spatial resolution for decay extraction. As well, it is desirable that, for a better validation of this type of methodology followed, it will be tried on other frescoes.

References

Andrienko N, Andrienko G (2005) Exploratory analysis of spatial and temporal data: a systematic approach. Springer, New York

Andrienko G, Andrienko N, Jankowski P, Keim D, Kraak M-J, MacEachren A, Wrobel S (2007a) Geovisual analytics for spatial decision support: setting the research agenda. Int J Geogr Inf Sci 21:839–857. https://doi.org/10.1080/13658810701349011

Andrienko G, Andrienko N, Wrobel S (2007b) Visual analytics tools for analysis of movement data. SIGKDD Explor Newsl 9:38–46. https://doi.org/10.1145/1345448.1345455

Avdelidis NP, Moropoulou A (2004) Applications of infrared thermography for the investigation of historic structures. J Cult Heritage 5:119–127

Bodnar L, Candoré JC, Nicolas JL, Szatanik G, Detalle V, Vallet JM (2012) Stimulated infrared thermography applied to help restoring mural paintings. J NDT&E Int 49:40–46

Candoré JC, Bodnar JL, Detalle V, Grossel P (2010) Non-destructive testing in situ, of works of art by stimulated infrared thermography. 15th international conference on photoacoustic and photothermal phenomena (ICPPP15) IOP Publishing. J Phys Conf Ser 214:012068. https://doi.org/10.1088/1742-6596/214/1/012068

Carlomagno GM, Di Maio R, Fedi M, Meola C (2011) Integration of infrared thermography and high-frequency electromagnetic methods in archaeological surveys. J Geophys Eng 8:93–105. https://doi.org/10.1088/1742-2132/8/3/S09

Conyers LB (2004) Ground-penetrating radar for archaeology. AltaMira, Walnut Creek

Danese M, Demšar U, Masini N, Charlton M (2010) Investigating material decay of historic buildings using visual analytics with multi-temporal infrared thermographic data. Archaeometry 52(3):482–501

De Mers MN (2002) GIS modeling in raster. Wiley, New York

Dumoulin J (2016) Infrared thermography: from sensing principle to nondestructive testing considerations. In: Soldovieri F, Masini N (eds) Sensing the past: from artifact to historical site. Springer, Berlin, pp 233–256

Faella G, Frunzio G, Guadagnuolo M, Donadio A, Ferri L (2012) The church of the nativity in Bethlehem: non-destructive tests for the structural knowledge. J Cult Heritage 13:27–41

Fiorelli G (1875) Descrizione di Pompei. Tipografia Italiana, Napoli

Getis A, Ord JK (1992) The analysis of spatial association by use of distance statistics. Geogr Anal 24(3):189–206

Goodman D, Piro S (2013) GPR remote sensing in archaeology, vol 9. Geotechnologies and the environment. Springer, New York

Grinzato E, Vavilov V, Kauppinen T (1998) Quantitative infrared thermography in buildings. Energy Build 29:1–9

Grinzato EP, Bressan C, Marinetti S, Bison PG, Bonacina C (2002a) Monitoring of the Scrovegni Chapel by IR thermography: Giotto at infrared. Infrared Phys Technol 43(3–5):165–169

Grinzato E, Bison PG, Marinetti S (2002b) Monitoring of ancient buildings by the thermal method. J Cult Heritage 3:21–29

Guarnieri M, Danielis A, Francucci M, Collibus M, Fornetti G, Mencattini A (2014) 3D remote colorimetry and watershed segmentation techniques for fresco and artwork decay monitoring and preservation. J Archaeol Sci 46:182–190

Inagaki T, Ishii T, Iwamoto T (1999) On the NDT and E for the diagnosis of defects using infrared thermography. NDT&E Int 32:247–257

Kandemir-Yucel A, Tavukcuoglu A, Caner-Saltik EN (2007) In situ assessment of structural timber elements of a historic building by infrared thermography and ultrasonic velocity. Infrared Phys Technol 49:243–248

Keim DA, Ward M (2003) Visualization. In: Berthold M, Hand DJ (eds) Intelligent data analysis. Springer, Berlin, pp 403–428

Kohonen T (1997) Self-organizing maps, 3rd edn. Springer, Berlin

Koloski-Ostrow AO (1990) The Sarno bath complex. Monografie (Italy. Soprintendenza archeologica di Pompei), 4, oma: “L’Erma” di Bretschneider

Lancaster LC (2015) Opus Caementicium. In: Innovative vaulting in the architecture of the Roman Empire. Cambridge University Press, Cambridge, pp 19–38. https://doi.org/10.1017/CBO9781107444935.003

Lanorte A, Danese M, Lasaponara R, Murgante B (2013) Multiscale mapping of burn area and severity using multisensor satellite data and spatial autocorrelation analysis. Int J Appl Earth Obs Geoinf 20:42–51. https://doi.org/10.1016/j.jag.2011.09.005

Leucci G, Masini N, Persico R, Soldovieri F (2011) GPR and sonic tomography for structural restoration: the case of the cathedral of Tricarico. J Geophys Eng 8(3):76–92. https://doi.org/10.1088/1742-2132/8/3/S08

MacEachren AM, Kraak MJ (2001) Research challenges in geovisualization. Cartogr Geogr Inf Sci 28:3–12. https://doi.org/10.1559/152304001782173970

Masini N, Soldovieri F (2017) Sensing the past: from artifact to historical site. Springer, Berlin. https://doi.org/10.1007/978-3-319-50518-3_1

Masini N, Nuzzo L, Rizzo E (2007) GPR investigations for the study and the restoration of the Rose Window of Troia Cathedral (Southern Italy). Near Surf Geophys 5(5):287–300. https://doi.org/10.3997/1873-0604.2007010

Masini N, Persico R, Rizzo E, Calia A, Giannotta MT, Quarta G, Pagliuca A (2010) Integrated techniques for analysis and monitoring of historical monuments: the case of S. Giovanni al Sepolcro in Brindisi (Southern Italy). Near Surf Geophys 8(5):423–432. https://doi.org/10.3997/1873-0604.2010012

Masini N, Sileo M, Leucci G, Soldovieri F, D'Antonio A, De Giorgi L, Pecci A, Scavone M (2017) Integrated in situ investigations for the restoration: the case of regio VIII in Pompeii. In: Masini N, Soldovieri F (eds) Sensing the past, vol 16. Geotechnologies and the environment. Springer, Cham, pp 557–586

Merello P, Beltrán P, García-Diego FJ (2016) Quantitative non-invasive method for damage evaluation in frescoes: Ariadne's House (Pompeii, Italy). Environ Earth Sci 75:165. https://doi.org/10.1007/s12665-015-5066-3

Nolè G, Lasaponara R, Lanorte A, Murgante B (2014) Quantifying urban sprawl with spatial autocorrelation techniques using multi-temporal satellite data. Int J Agric Environ Inf Syst 5(2):20–38. https://doi.org/10.4018/ijaeis.2014040102

O'Sullivan D, Unwin D (2002) Geographic information analysis. Wiley, New York

Pérez-Gracia V, Caselles JO, Clapés J, Martinez G, Osorio R (2013) Non-destructive analysis in cultural heritage buildings: evaluating the Mallorca cathedral supporting structures. NDT&E Int 59:40–47

Persico R (2014) Introduction to ground penetrating radar: inverse scattering and data processing. Wiley, New York

Rangayyan RM, Acha B, Serrano C (2011) Colour image processing with biomedical applications. Society of Photo-Optical Instrumentation Engineers (SPIE)

Soldovieri F, Orlando L (2009) Novel tomographic based approach and processing strategies for GPR measurements using multifrequency antennas. J Cult Heritage 10:83–92

Tomlin CD (1990) Geographic information systems and cartographic modeling. Prentice Hall, Englewood Cliffs